

# 1 A hybrid and poly-polish workflow for 2 the complete and accurate assembly 3 of phage genomes: a case study of 4 ten *Przondoviruses*

5

6 **Claire K. A. Elek<sup>1,2</sup>, Teagan L. Brown<sup>1</sup>, Thanh Le Viet<sup>1</sup>, Rhiannon Evans<sup>1</sup>, David J. Baker<sup>1</sup>,**  
7 **Andrea Telatin<sup>1</sup>, Sumeet K. Tiwari<sup>1</sup>, Haider Al-Khanaq<sup>1</sup>, Gaëtan Thilliez<sup>1</sup>, Robert A.**  
8 **Kingsley<sup>1,2</sup>, Lindsay J. Hall<sup>1,2,3</sup>, Mark A. Webber<sup>1,2</sup>, Evelien M. Adriaenssens<sup>1\*</sup>**

9

10 <sup>1</sup> Quadram Institute Bioscience, Rosalind Franklin Road, Norwich Research Park, Norwich,  
11 UK

12 <sup>2</sup> University of East Anglia, Norwich Research Park, Norwich, UK

13 <sup>3</sup> Chair of Intestinal Microbiome, ZIEL—Institute for Food and Health, School of Life Sciences,  
14 Technical University of Munich, Freising, Germany

15 \* Correspondence: [evelien.adriaenssens@quadram.ac.uk](mailto:evelien.adriaenssens@quadram.ac.uk)

16 **Keywords:** *Klebsiella*; bacteriophage; phage; *Przondovirus*; sequencing; assembly.

17 **Abbreviations:** BHI, brain heart infusion; CPS, capsular polysaccharide; DNAP, DNA  
18 polymerase; DTR, direct terminal repeat; HYPPA, hybrid and poly-polish phage assembly;  
19 ICTV, International Committee on Taxonomy of Viruses; LPS, lipopolysaccharide; NCBI,  
20 National Centre for Biotechnology Information; MLST, multilocus sequence typing; ONT,  
21 Oxford Nanopore Technologies; PEG, polyethylene glycol; QC, quality control; QIB, Quadram  
22 Institute Bioscience; RNAP, RNA polymerase.

23

24

25

26

## 27 ABSTRACT

28 Bacteriophages (phages) within the *Przondovirus* genus are T7-like podoviruses belonging  
29 to the *Studiervirinae* subfamily, within the *Autographiviridae* family and have a highly  
30 conserved genome organisation. The genome size of these phages ranges from 37 kb to 42  
31 kb, encode 50-60 genes and are characterised by the presence of direct terminal repeats  
32 (DTRs) flanking the linear chromosome. These DTRs are often deleted during short-read-only  
33 and hybrid assemblies. Moreover, long-read-only assemblies are often littered with  
34 sequencing and/or assembly errors and require additional curation. Here, we present the  
35 isolation and characterisation of ten novel *przondoviruses* targeting *Klebsiella* spp. We  
36 describe HYPPA – a HYbrid and Poly-polish Phage Assembly workflow, which utilises long-  
37 read assemblies in combination with short-read sequencing to resolve phage DTRs and  
38 correcting errors, negating the need for laborious primer walking and Sanger sequencing  
39 validation. Our data demonstrate the importance of careful curation of phage assemblies  
40 before publication, and prior to using them for comparative genomics.

## 41 IMPACT STATEMENT

42 The current workflows employed for phage genome assembly are often error-prone and  
43 can lead to many incomplete phage genomes being deposited within databases. This can  
44 create challenges when performing comparative genomics, and may also lead to incorrect  
45 taxonomic assignment. To overcome these challenges we proposed HYPPA, a workflow that  
46 can produce complete and high-quality phage genomes without the need for laborious lab-  
47 based validation.

## 48 DATA SUMMARY

49 Phage raw reads are available from the National Centre for Biotechnology Information  
50 Sequence Read Archive (NCBI-SRA) under the BioProject number PRJNA914245. Phage  
51 annotated genomes have been deposited at GenBank under the accessions OQ579023-  
52 OQ579032 (**Table 1**). Bacterial WGS data for clinical preterm infant samples have been  
53 deposited at GenBank under BioProject accession PRJNA471164 (**Table S1**). Bacterial raw  
54 reads for food samples are available from NCBI-SRA with individual accessions  
55 (SAMN33593347-SAMN33593351), and can be found under the BioProject number  
56 PRJNA941224 (**Table S1**). Strain-specific details for bacteria and publicly-available phages  
57 used in these analyses, along with accessions for the latter can be found in **Table S1** and  
58 **Table S6**, respectively. The CL1-CL8 clinical *Klebsiella* strains (**Table S1**) were under a  
59 Materials Transfer Agreement, for which sequencing data and strain information is not  
60 available.

## 61 INTRODUCTION

62 Double-stranded (ds) DNA bacteriophages with the characteristic head-tail morphology,  
63 also known as tailed phages, are a diverse group of viruses spanning 47 families, 98  
64 subfamilies, and 1197 genera, with many more being unclassified (1-4). Phages within the  
65 *Przondovirus* genus are T7-like podoviruses, meaning they have a short tail morphotype,  
66 belonging to the *Studiervirinae* subfamily, within the *Autographiviridae* family (5). T7-like  
67 phages are renowned for following a strictly lytic life cycle, with the eponymous *Escherichia*  
68 *coli* phage T7 often used as the type isolate to represent the *Autographiviridae* family (6, 7).

69 *Autographiviridae* phages typically have genomes ranging from 37 to 42 kb in size and  
70 encode 50-60 genes, with the DNA-directed RNA polymerase (RNAP) being a hallmark of the  
71 family (5, 6, 8). The genome organisation of genera within the *Studiervirinae* subfamily is  
72 highly conserved: all genes are unidirectional and show a high degree of synteny (2, 5-7).

73 Tailed phages employ a remarkably diverse array of packaging methods that generate  
74 distinct termini (9, 10). The termini of T7-like phages consist of direct terminal repeats (DTRs)  
75 of varying lengths that flank the genome (6). The DNA of T7-like phages is concatemeric when  
76 generated within the bacterial cell and requires the assistance of terminases to cut at specific  
77 sites to package the DNA into the procapsid (9-11). Whilst each concatemer contains a single  
78 copy of the repeat, a second repeat is synthesised at the other end of the genome to prevent  
79 loss of genetic material (9, 12). Additionally, the DTRs are thought to prevent host-associated  
80 digestion *in vivo* and assist in DNA replication during phage infection (10, 13).

81 Many phage genomes deposited within public sequence databases are incomplete, often  
82 with DTR sequences missing or simply not annotated. Thus, our relatively limited  
83 understanding of phage biology is exacerbated by incomplete data and can make  
84 classification and comparative genomics more challenging (14). Indeed, high-quality genomic  
85 data will help identify relationships between taxonomic classification, infection kinetics, and  
86 phage-host interactions that are essential to the use of phages as therapeutics (14).

87 The genus *Klebsiella* comprises a heterogenous group of Gram-negative bacteria in the  
88 Enterobacteriales order (15). *Klebsiella* spp. are common commensals of human mucosae,  
89 presenting a major risk factor for developing invasive disease and are therefore important  
90 opportunistic pathogens (15, 16). Antibiotic resistance among *Klebsiella* spp. represents a  
91 major threat to human health, with many isolates now multidrug resistant (15, 16). Therefore,  
92 conventional treatment using currently available antibiotics is becoming increasingly  
93 ineffective, and combined with no new antibiotics in the drug development pipeline, we are  
94 entering a post-antibiotic era (17, 18). Treatment of recalcitrant infections with bacterial  
95 viruses, bacteriophage therapy, has seen a resurgence in recent years as an alternative or  
96 adjunctive to current antibiotic therapy (19, 20).

97 Phage isolation involves monomicrobial or polymicrobial enrichment that often selects for  
98 the fittest phages (14, 21-23). Indeed, the rapid infection cycle of T7-like phages means that  
99 they are often overrepresented following traditional isolation methods (14, 21, 23). Here, ten  
100 novel T7-like phages belonging to the *Przondovirus* genus in the *Autographiviridae* family have  
101 been isolated against four *Klebsiella* strains belonging to different species, and characterised.  
102 Hybrid poly-polish assembly methods have recently been described for assembling bacterial  
103 genomes (24). Here we developed and validated a similar approach to ensure accurate and  
104 complete phage genome assembly, in a new workflow HYPPA – a HYbrid and Poly-polish  
105 Phage Assembly which was tested and validated for these new phages. The workflow utilises  
106 long-read assemblies in combination with short-read sequencing to resolve phage DTRs and  
107 correct sequencing and/or assembly errors, which negates the need for laborious primer  
108 walking and Sanger sequencing validation.

## 109 MATERIALS AND METHODS

### 110 Bacterial strains and growth conditions

111 Where specified, *Klebsiella* spp. used here were derived from previous studies (25-29) and  
112 are listed in **Table S1**. All *Klebsiella* strains were cultured overnight on brain heart infusion  
113 (BHI) agar (Oxoid) at 37°C. Liquid cultures were prepared by inoculation of 10 mL BHI broth  
114 with each bacterial strain and incubated at 37°C with shaking at 200 rpm for 3 h. Single colony  
115 variants were identified on solid media by changes in colony morphology and were purified by  
116 selecting a single colony for three successive rounds of purification on MacConkey no. 3 agar  
117 (Oxoid), and incubated overnight at 37°C.

### 118 Preparation of bacterial DNA and sequencing

119 Genomic DNA for each *Klebsiella* strain was extracted using the AllPrep Bacterial  
120 DNA/RNA/Protein kit (QIAGEN) according to the manufacturer's instructions. DNA was  
121 quantified as previously described and normalised to 5 ng  $\mu$ L $^{-1}$ .

122 DNA was prepared using the Illumina DNA Prep library preparation kit and was whole-  
123 genome sequenced on the Illumina NextSeq500 platform generating 2 x 150 bp paired-end  
124 reads by QIB Sequencing Core Services.

125 Additionally, *K. michiganensis* M7 21 2 #35, *K. pneumoniae* M26 18 1, *K. pneumoniae* M26  
126 18 2 #21 KpnN, *K. pneumoniae* M26 18 2 #21 KpnA, and *K. pneumoniae* ST38 01 were  
127 prepared for enhanced sequencing according to the sequence facilities instructions  
128 (MicrobesNG). Genomes were provided assembled and annotated by MicrobesNG.

129 **Bacterial genomics**

130 Short-read data provided without pre-processing by QIB Sequencing Core Services was  
131 QC filtered, trimmed, assembled, annotated, and analysed using the ASA<sup>3</sup>P v1.2.2 (30), or  
132 Bactopia v1.6.4 (31) pipelines. Preliminary strain designations were determined by ribosomal  
133 multilocus sequence typing (rMLST) (<https://pubmlst.org/species-id>) (32). The PubMLST  
134 database (<https://pubmlst.org/>) (33) was used to determine sequence type (ST) for *K. oxytoca*  
135 species complex and *K. aerogenes*, while the Institute Pasteur MLST database  
136 (<https://bigsdb.pasteur.fr/>) was used to determine sequence types of *K. pneumoniae* species  
137 complex. The capsular type for each strain was predicted using Kleborate (34) and Kaptive  
138 (35) on the QIB Galaxy platform, and those with a match confidence of good or higher were  
139 included.

140 **Isolation and single-plaque purification of phages**

141 Samples from various UK wastewater treatment plants were screened for *Klebsiella*-  
142 specific phages using a range of *Klebsiella* strains as hosts for enrichment, adapted from Van  
143 Twest *et al.* (36). Briefly, 300 µL filtered wastewater was mixed with 60 µL exponential bacterial  
144 culture and used to inoculate 5 mL BHI broth. Enrichments were incubated overnight at 37°C  
145 with shaking at 200 rpm. Enrichments were then centrifuged (4000 x g for 15 min) and passed  
146 through a 0.45 µm filter before spot testing by double agar overlay plaque assay, as previously  
147 described (37). All incubations for overlay method were performed over 4-17 h at 37°C. Single  
148 plaque purifications were made by extracting single plaques from the soft agar layer using  
149 sterile toothpicks and suspended in approximately 300 µL BHI broth. Suspensions were  
150 centrifuged (13,000 x g for 5 min) and supernatant collected. Ten-fold serial dilutions of the  
151 supernatant were performed in phage buffer (75 mM NaCl; 10 mM MgSO<sub>4</sub>; 10 mM Tris, pH  
152 7.5; 0.1 mM CaCl<sub>2</sub>) and 10 µL of each dilution plated onto double agar overlay and incubated  
153 as described above. This process was repeated at least three times to create phage stocks.

154 Phage amplification was performed as for single plaque purification in BHI broth. Once  
155 supernatant was collected, approximately 100 µL of phage suspension was spread onto three  
156 double agar overlay plates and incubated as before. Phage stocks were prepared by  
157 extraction of phage clearance zones. This was achieved by removal of the soft agar layer,  
158 which was resuspended in phage buffer, and centrifuged (4000 x g for 15 min). Phage  
159 supernatant was passed through a 0.45 µm filter into a sterile glass universal and stored at  
160 4°C.

161 **Phage host range**

162 Phage host range was tested by plaque assay as described above on a range of clinical,  
163 wastewater, food, and type strain *Klebsiella* spp. as described previously (38). Only assays  
164 where individual plaques were identified were recorded as positive.

165 **Phage DNA extraction and whole-genome sequencing**

166 Phage virions were concentrated by polyethylene glycol (PEG) 8000 (Thermo Fisher)  
167 precipitation for DNA extraction. Briefly, phage stock was treated with 1  $\mu$ L DNase I (10 U  $\mu$ L $^{-1}$ )  
168 (Merck) and 1  $\mu$ L RNase A (10 U  $\mu$ L $^{-1}$ ) (Merck) per mL of stock and incubated at 37°C for  
169 30 min. PEG precipitation was performed with PEG 8000 (10% w/v) and 1 M NaCl and  
170 incubated overnight at 4°C. The precipitate was centrifuged (17,000  $\times g$  for 10 min) and  
171 resuspended in 200  $\mu$ L nuclease-free water. Resuspended phage pellets were treated with  
172 proteinase K (50  $\mu$ g mL $^{-1}$ ) (Merck), EDTA (final concentration 20 mM), and 10% SDS (final  
173 concentration 0.5% v/v) and incubated at 55°C for 1 h.

174 DNA was extracted using the Maxwell® RSC Viral Total Nucleic Acid Purification kit  
175 (Promega), as per the manufacturer's instructions into nuclease-free water. Phage DNA was  
176 quantified by Qubit 3.0 fluorometer using the high sensitivity dsDNA kit (Invitrogen). DNA was  
177 prepared using Illumina DNA Prep (formerly Nextera Flex) library preparation kit and was  
178 whole-genome sequenced on the Illumina NextSeq500 platform generating 2 x 150 bp paired-  
179 end reads by QIB Sequencing Core Services. MinION libraries (Oxford Nanopore  
180 Technologies, ONT) were constructed without shearing using the short fragment buffer and  
181 loaded onto the R9.4.1 flow cell according to the manufacturer's instructions by QIB  
182 Sequencing Core Services.

183 Both long-read and short-read raw data for all ten przondoviruses were deposited in NCBI  
184 under BioProject number PRJNA914245.

185 **Phage genomics**

186 *Assembly and annotation*

187 All quality control, pre-processing, assembly, and annotation of phage genomes were  
188 performed on the QIB Galaxy platform.

189 We checked short-read data for quality using fastQC v0.11.8 (39). Based on this fastQC  
190 analysis, reads were pre-processed with fastp v0.19.5 (40), using a hard trim of between 4  
191 and 10 bases on both the front and tail to retain at least a per base quality of 28.

192 Long-read data was demultiplexed following sequencing and quality checked with  
193 NanoStat v0.1.0 (41). Pre-processing was performed as part of the assembly, and assembled  
194 using Flye v2.9 (42) with default settings, which included correction and trimming of reads.  
195 Flye was used in the first instance as previously published work has determined it is the most

196 accurate and reliable assembler (43-45). Where Flye was unable to generate a high-quality  
197 assembly, Canu v2.2 (46) was used as an alternative. Error correction and trimming were  
198 performed as part of the default settings when assembling using Flye or Canu. Flye  
199 additionally performed one iteration of long-read polishing by default. We assembled all  
200 phages with and without trimming adapter/barcode sequences for long-reads. Trimming was  
201 performed with Porechop v0.2.3 (<https://github.com/rrwick/Porechop>) (47) with default  
202 settings.

203 We performed several iterations of long-read and short-read polishing on long-read-only  
204 assemblies in a specific order. Firstly, two iterations of long-read polishing were performed  
205 using Medaka (48) with default settings, using the previous polished data as the input for the  
206 next round of polishing. Secondly, one iteration of short-read polishing was performed using  
207 Polypolish (49) with default settings. Finally, a second iteration of short-read polishing was  
208 performed using POLCA (50) with default settings. We used raw reads for each iteration of  
209 long-read polishing and pre-processed reads for each iteration of short-read polishing.

210 Prior to development of the current phage assembly workflow, we had adopted a few other  
211 methodologies for resolving the genomes. One method was short-read-only assembly, where  
212 phages were assembled *de novo* using Shovill v1.0.4 (<https://github.com/tseemann/shovill>)  
213 with default settings (51, 52). Briefly, trimming was disabled by default and manual trimming  
214 was performed as part of the pre-processing step prior to assembly. Additionally, SPAdes was  
215 used as the default assembler within the Shovill pipeline. We attempted short-read polishing  
216 of long-read-only data using Pilon v1.20.1 (53) with default settings. Where specified, we also  
217 performed hybrid assembly using raw long-read and pre-processed short-read data, as  
218 previously described using Unicycler v0.4.8.0 (54) with default settings. Porechop v0.2.3  
219 (<https://github.com/rrwick/Porechop>) (47) was used for *Klebsiella* phage Oda only. All  
220 assembly details are given in **Tables S3-S5**.

221 Following assembly, the contigs were manually checked for DTRs flanking the genome, as  
222 well as with PhageTerm (55) which was unable to identify the DTRs since it does not work  
223 well for Nextera-based sequence libraries. Where we could not determine the length and  
224 sequence of the DTRs, we performed primer walking. Outward-facing primers were designed  
225 to “walk” the genome termini using Sanger sequencing (56). Phage DNA was extracted, and  
226 for each phage at least two primers were designed for the reverse strand to walk the beginning  
227 of the genome and identify the left terminal repeat, and at least two primers were designed for  
228 the forward strand to walk the end of the genome to identify the right terminal repeat. The  
229 phage DNA and each primer were then sent for Sanger sequencing separately (Eurofins,  
230 Germany). Sanger sequences were visualised in FinchTV v1.5.0  
231 (<https://digitalworldbiology.com/FinchTV>) and compared to the reference phage genome, and

232 DTRs annotated using the Molecular Biology suite on the Benchling platform  
233 (<https://www.benchling.com/>).

234 Assemblies generating multiple contigs were checked for contamination using Kraken 2  
235 v2.1.1 (57).

236 Verification of the DTRs and assessment of assembly quality was performed by mapping  
237 the raw reads back to the assembled genome using Bowtie 2 v2.3.4.3 (58) and visualised  
238 using IGV v2.7.2 (59), and variant calling performed using iVar v1.0.1 (60). Additionally, BWA-  
239 MEM v0.7.17.1 (<https://github.com/lh3/bwa>) was used to map long-reads back to the  
240 reference using default settings optimised for ONT reads (61, 62).

241 Assemblies in the reverse orientation were reorientated by reverse complementation of the  
242 genome in UGENE v38.0 (63) and uploaded to Benchling. Contigs were then reoriented to  
243 begin at the same start point, based on well-curated reference phages and the analysis of the  
244 DTRs.

245 Genome annotation was performed using Pharokka v1.2.1 with default settings  
246 (<https://github.com/gbouras13/pharokka>) (64). Specifically, coding sequences were predicted  
247 with PHANOTATE (65).

#### 248 *Comparative genomics*

249 Where specified, publicly-available phage genomes used for comparative genomics were  
250 derived from these studies (20, 66-78), listed in **Table S6**, and downloaded from the GenBank  
251 database.

252 The closest relative for each phage was determined as the top hit according to maximum  
253 score identified by nucleotide BLAST (BLASTn) (<https://blast.ncbi.nlm.nih.gov/Blast.cgi>) and  
254 optimised for somewhat similar sequences (79). Genes associated with specific phage  
255 families were identified and used for preliminary taxonomic assignment. Alignments were  
256 performed using Mauve v20150226 (80) between the closest relative and phages from the  
257 same genera. The intergenomic similarity between przondoviruses in the collection and a  
258 selection of publicly-available related phages was calculated using VIRIDIC on the web server  
259 (<http://rhea.icbm.uni-oldenburg.de/VIRIDIC/>) (81).

260 Phylogenetic analyses were performed using the hallmark DNA-directed RNA polymerase  
261 (RNAP) amino acid sequence for all phages and a selection of publicly-available  
262 phylogenetically-related phages downloaded from the NCBI protein database  
263 (<https://www.ncbi.nlm.nih.gov/>). Multisequence alignment of the RNAP amino acid sequences  
264 was performed using the MUSCLE algorithm in MEGA X v10.0.5 (82) with default settings. A  
265 maximum-likelihood tree was generated with 500 bootstraps using the default Jones-Taylor-  
266 Thornton model. Phylogenetic analysis was performed using 35 amino acid sequences, with

267 a total of 684 positions in the final analysis. Tree image rendering was performed using iTOL  
268 v6.1.1 (<https://itol.embl.de/>) (83).

269 Linear mapping of coding sequences for phage final assemblies was performed using  
270 Clinker v.0.0.23 (84).

## 271 **RESULTS AND DISCUSSION**

### 272 **Phage isolation and host range determination**

273 In this study, we isolated ten lytic T7-like phages from a variety of river water and  
274 wastewater samples, using four different *Klebsiella* spp. as isolation hosts (**Table 1**). To  
275 examine the host range, we tested the ten phages against a collection of *Klebsiella* spp. from  
276 different sources, representing a range of capsule and sequence types. All phages had a  
277 narrow host range, with seven being able to infect only a single *Klebsiella* strain within our  
278 collection (**Fig. 1**).

279 Three of the ten przondoviruses were used to test and validate the HYPPA workflow: Oda,  
280 Toyotomi, and Tokugawa. As the three unifiers of the HYPPA workflow, these were named  
281 after the three unifiers of Japan (see **Development of a new workflow for the assembly of**  
282 **complete phage genomes**).

283 Only three of our phages were capable of productively infecting more than one *Klebsiella*  
284 strain. *Klebsiella* phage Toyotomi was able to infect two different species; a *K. michiganensis*  
285 strain (its isolation host) and a *K. quasipneumoniae* strain. *Klebsiella* phages Emom and  
286 Amrap were both able to infect two different isolates of *K. oxytoca*. *Klebsiella* phage Whistle  
287 was the only phage capable of productively infecting four strains of *Klebsiella*, spanning three  
288 different species (*K. grimontii*, *K. michiganensis*, and *K. variicola*), and caused lysis without  
289 productive infection on a further three *K. pneumoniae* isolates. We could not establish a link  
290 between capsular type and host range for these phages.

291 Przondoviruses and other T7-like phages have a relatively small genome of 37 to 42 kb,  
292 and this may limit their host expansion capabilities (for taxonomic assignment of the ten  
293 phages in this study, see section **Phage genome characterisation and taxonomy**).  
294 However, Whistle was capable of infecting multiple hosts, along with Emom, Amrap, and  
295 Toyotomi. Previous work has shown that T7-like phages are capable of infecting multiple hosts  
296 (66) and that host range is determined by interaction between phage receptor binding proteins,  
297 i.e. tail fibre and/or spike proteins, and bacterial cell receptors (14, 66, 85). LPS components  
298 are almost always identified as the secondary receptor for irreversible attachment in Gram-  
299 negative-targeting podoviruses (6, 14). Whether initial interaction with the outer membrane  
300 and degradation of the CPS constitutes a *bona fide* reversible attachment step, or whether

**Table 1.** Przondoviruses within the collection to date and data relating to the closest database relative.

Phage Name	Source	Isolation host	Genome size (bp)	GC content (%)	DTR size (bp)	No. CDS	Accession	Closest database relative according to BLASTn		
								Name	Coverage (%)	ID (%)
Oda	River water	K.mi.	41,642	52.64	181	58	OQ579023	<i>Klebsiella</i> phage SH-KP152226	92.0	94.62
Toyotomi	Wastewater	K.mi.	41,268	52.64	180	55	OQ579024	<i>Klebsiella</i> phage SH-KP152226	92.0	94.71
Mera	Wastewater	K.mi.	41,400	52.58	180	56	OQ579025	<i>Klebsiella</i> phage SH-KP152226	92.0	94.34
Speegle	Wastewater	K.mi.	41,395	52.64	180	58	OQ579026	<i>Klebsiella</i> phage SH-KP152226	93.0	94.70
Cornelius	Wastewater	K.mi.	40,437	52.72	180	55	OQ579027	<i>Klebsiella</i> phage SH-KP152226	94.0	94.84
Tokugawa	Wastewater	K.mi.	41,414	52.64	181	56	OQ579028	<i>Klebsiella</i> phage SH-KP152226	92.0	94.70
Saitama	Wastewater	K.qp.	40,741	53.06	181	51	OQ579029	<i>Klebsiella</i> phage K11	96.0	95.71
Emom	Wastewater	K.ox.	40,788	52.56	183	53	OQ579030	<i>Klebsiella</i> phage KP32	94.0	93.14
Amrap	Wastewater	K.ox.	41,209	52.47	182	57	OQ579031	<i>Klebsiella</i> phage KPN3	85.0	95.05
Whistle	Wastewater	K.va.	40,735	52.40	181	54	OQ579032	<i>Klebsiella</i> phage IME264	94.0	94.78

K.mi., *K. michiganensis* M7 21 2 #21; K.ox., *K. oxytoca* M59 22 8; K.qp., *K. quasipneumoniae* P057K W; K.va., *K. variicola* DSM15968. CDS, coding sequences. Bacterial host species accessions are given in **Table S2**.

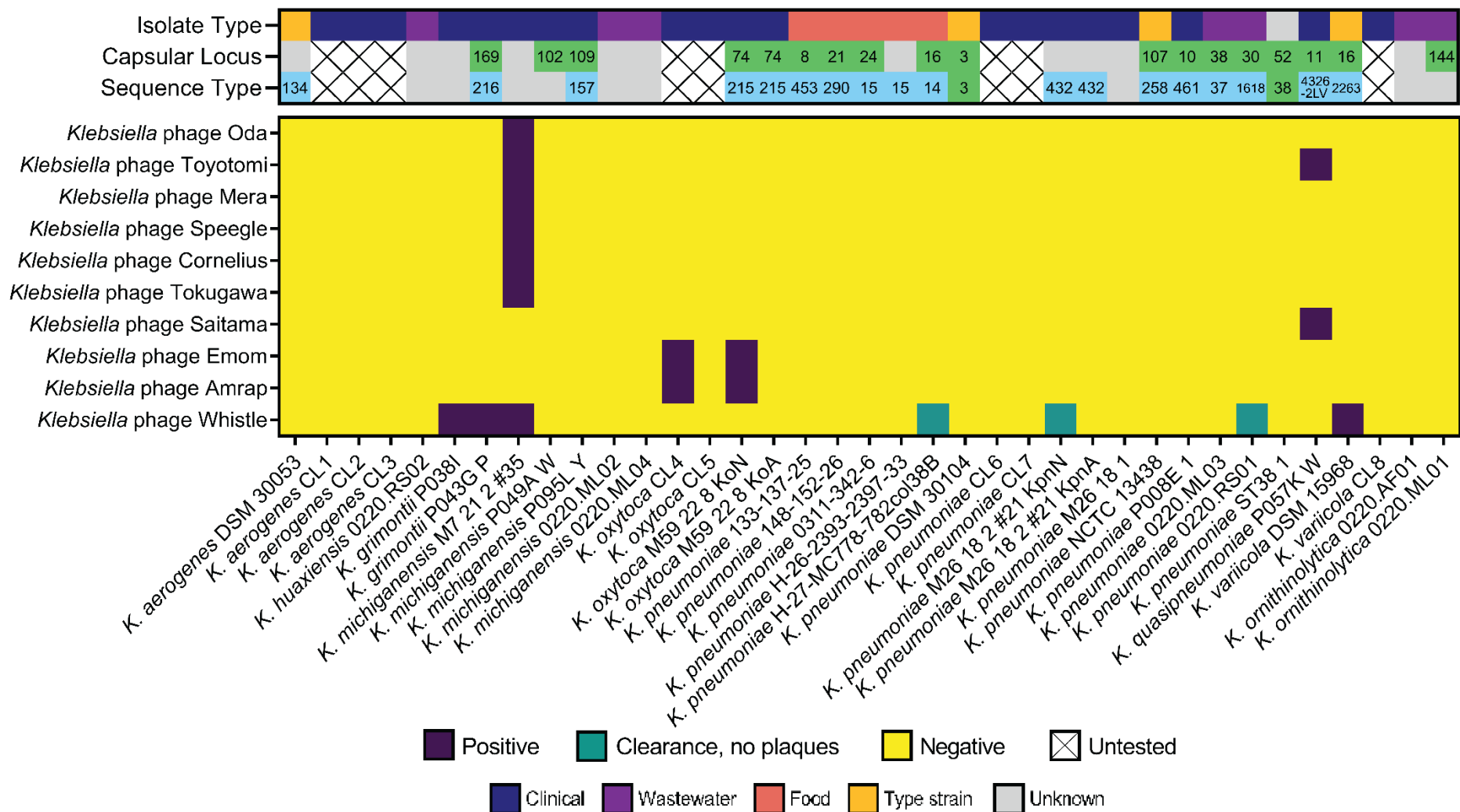


**Fig. 1. Heatmap for host range of the przondoviruses in the collection by plaque assay against a diverse range of *Klebsiella* spp.** Top panel, isolate type, capsular type, and sequence type. The source of each isolate is given as isolate type, with grey being unknown source. Capsular loci determined by Kaptive and/or Kleborate, green; unknown or no match confidence, grey. Sequence type (ST) determined by multilocus sequence typing, blue; unknown or incomplete matches, grey. No sequencing data available, untested. Bottom panel, host range heatmap. Productive infection (positive) is the observation of individual plaques, purple; lysis without productive infection is the observation of clearance without individual plaques, green; no productive infection or clearance (negative), yellow.

304 this is a prerequisite to reversible attachment by the phage to another outer membrane  
305 component is yet to be fully elucidated (6, 14, 86, 87).

306 Some phages can be “trained” to increase their host range through co-evolution assays  
307 (19, 88). This may be particularly useful in cases of lysis from without, such as observed in  
308 Whistle, as they are already capable of binding to host receptors but unable to cause  
309 productive infection.

310 Intriguingly, Toyotomi was the only phage capable of infecting two different *Klebsiella*  
311 species, that none of its closest relatives from our collection were capable of infecting, despite  
312 exceptionally high protein sequence similarity across their tail fibre proteins.

313 Multiple factors affect host range and broadly involve extracellular and intracellular  
314 mechanisms. Extracellular mechanisms involve the ability of phages to bind to specific phage  
315 receptors on the bacterial cell surface that facilitate DNA ejection (89). Intracellular  
316 mechanisms involve evasion of phage defence systems that facilitate phage propagation (89).  
317 Expression of diffusible depolymerases facilitate interaction of phages with their primary and  
318 secondary receptor. This extracellular mechanism is more likely to explain the ability of Whistle  
319 to infect more than one isolate since there is productive infection. Thus, the ability of several  
320 przondoviruses in our collection to infect different *Klebsiella* isolates could indicate that they  
321 share similarities in the chemical composition of their capsules, enabling degradation by a  
322 single depolymerase and allowing access to the phage receptors on the bacterial cell.  
323 Moreover, the bacterial isolates could share similar sugar motifs within their LPS structures,  
324 which are thought to be the secondary receptor of phages within the *Autographiviridae* family  
325 (6).

### 326 **Development of a new workflow for the assembly of complete phage genomes**

327 To generate complete and accurate genomes for these ten phages, which included  
328 resolving the defined ends of phage genomes, and correcting sequencing and/or assembly  
329 errors, we utilised a long-read-only assembly with sequential polishing steps. This  
330 methodology exploited both long-read and short-read sequencing data in a workflow that we  
331 have named HYPPA – HYbrid and Poly-polish Phage Assembly (see also **Materials and**  
332 **Methods**) before moving onto annotation and comparative genomics (**Fig. 2**). Firstly, the long-  
333 reads were assembled using Flye or Canu, followed by two iterations of long-read polishing  
334 with Medaka. Next, we performed two iterations of short-read polishing using Polypolish (for  
335 the first iteration) and POLCA (for the second iteration).

336 Initially, Flye was used as the primary assembler in our HYPPA workflow and worked  
337 particularly well for phages with both very high sequence read coverage (Toyotomi at  
338 >117,000x) and very low sequence read coverage, which included Mera (8x), Speegle (23x),  
339 and Amrap (27x) (**Table S2**). However, Canu performed better with the other phages as the

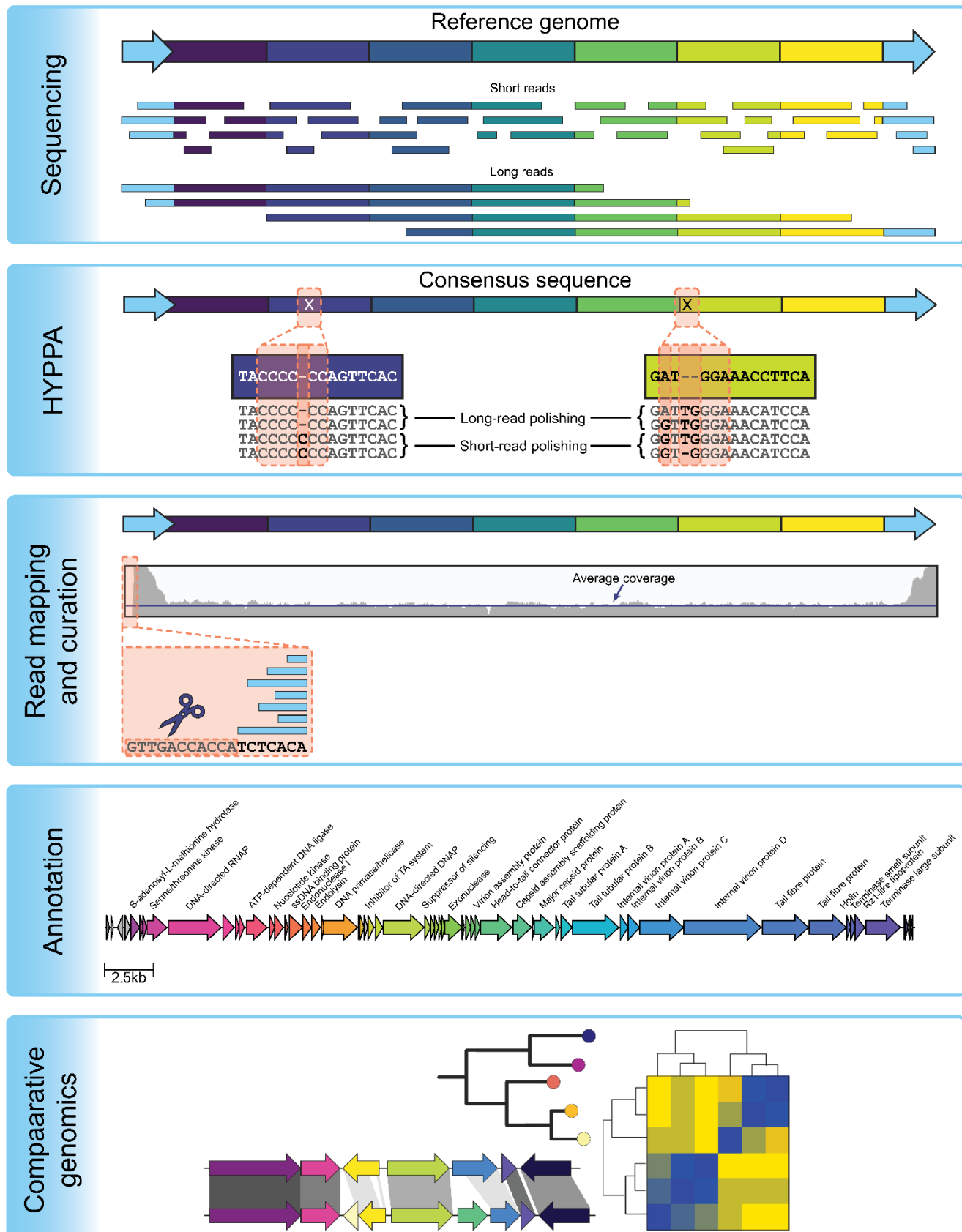
340 assemblies in general contained fewer errors. This is contrary to previously published literature  
341 that found Flye was more the more accurate assembler using default settings (43-45).

342 As an illustration of the HYPPA workflow, we provided a more detailed description of the  
343 process for phage Oda as an exemplar, for which the DTRs were validated with primer  
344 walking. Firstly, Oda was assembled using Canu, which yielded one contig of 41,761 bp. After  
345 two iterations of long-read polishing followed by two iterations of short-read polishing, the  
346 resulting contig was 41,769 bp in size. We were able to identify the terminal repeat regions,  
347 but both were flanked by a 64 bp sequence upstream of the left terminal repeat, and  
348 downstream of the right terminal repeat after all polishing iterations were complete. The two  
349 64 bp sequences were inverted repeats containing adapter sequences of 23 bp, with the  
350 remaining sequence being Nanopore barcodes which were manually removed. HYPPA was  
351 then used for phage Tokugawa, which after short-read only assembly had included a 79 bp  
352 repeat within the genome, but outside of the presumed DTR region (**Fig. S1**). Using HYPPA,  
353 the repeat was determined to be an assembly artefact and removed from the assembly. The  
354 final curated assembly for phages Oda and Tokugawa was 41,642 bp and 41,414 bp,  
355 respectively. Terminal repeats were present for both phages and complete at 181 bp, validated  
356 by primer walking and Sanger sequencing (**Fig. S1**).

357 We trimmed the long-reads using Porechop in an attempt to remove the adapter/barcode  
358 sequences, but when phage Oda was reassembled and polished using the trimmed reads,  
359 the right terminal repeat was missing three bases, but no other single nucleotide  
360 polymorphisms (SNPs) or indels were identified.

361 The HYPPA workflow without Porechop-mediated trimming was repeated for the remaining  
362 eight przondoviruses, resulting in final genome assemblies ranging between 40-42 kb (**Table**  
363 **1**). HYPPA was able to generate a complete genome for phage Toyotomi, where short-read-  
364 only, long-read-only, and hybrid assemblies were unable to do so and resulted in fragmented  
365 assemblies. Although our HYPPA workflow is a hybrid assembly approach, there is a clear  
366 distinction between this and traditional hybrid assembly methods. Importantly, HYPPA used  
367 the short-reads for polishing only, not during the genome assembly, whereas traditional hybrid  
368 assemblies utilise both long-read and short-read data during the assembly process itself.  
369 Moreover, short-read polishing of a long-read-only assembly using Pilon was also unable to  
370 resolve the genome of Toyotomi: partial repeat regions were found at the termini but were  
371 incomplete, and multiple errors within coding regions persisted. Using HYPPA, we were able  
372 to not only preserve the DTRs of Toyotomi, but also correct persistent sequencing and/or  
373 assembly errors that occurred in all non-HYPPA assemblies.

374 The genome organisation of genera within the *Autographiviridae* family is highly conserved:  
375 all genes are unidirectional and show a high degree of synteny, and genomes are flanked by  
376 DTRs (2, 5-7). The DTRs of the przondoviruses described here were 180-183 bp in size,



377 **Fig. 2. Workflow for phage genome assembly and analysis.** Both long-read and short-read sequencing are recommended, followed by our HYPPA workflow for high quality phage genome assembly. Read mapping for short-read data and manual curation can correct any errors that were missed during polishing, followed by annotation and then comparative genomics.

378 demonstrating sequence similarity of 84.3-99.7%. DTRs are thought to assist circularisation  
379 of the phage genome once in the host cytoplasm to prevent host-induced enzymatic digestion  
380 (13). Thus, resolution of the DTRs is integral to accurate genomics and understanding of the  
381 biology of different phages.

382 **Comparison of HYPPA with traditional short-read-only assembly**

383 When compared to typical short-read-only methodologies of phage genome assembly, in our  
384 case using Shovill (51), the HYPPA workflow required significantly less manual curation (**Fig.**  
385 **2**). Typically, phage genomes are assembled using short-read only data, and many of these  
386 genomes are then published without additional curation, leaving them with potentially  
387 significant sequencing and/or assembly errors. Using short-read-only assembly methods for  
388 our collection of przondoviruses, we observed that some were in the reverse orientation rather  
389 than the forward orientation as is expected for 50% of the assemblies, and some had the  
390 DTRs assembled in the middle of the contig. Addressing these issues required manually re-  
391 orienting the assemblies and ensuring they all had the same start position, as suggested in  
392 the Phage Annotation Guide (90). In contrast, the HYPPA workflow resulted in assemblies  
393 with correct start and stop sites, but some were still in the reverse orientation.

394 To check for DTRs in short-read only assemblies, we initially looked for increased reads  
395 within the read mapping profiles, which are distinguished by one or two large peaks, and can  
396 be automated using the tool PhageTerm (55). If a single peak was observed anywhere other  
397 than at either end of the assembly, the assembly had been opened in the middle of the genome  
398 and required each to be re-oriented to have the same starting position.

399 Incorrect orientation is a feature of phage genome assembly, and with short-read-only data  
400 in particular, may be artificially linearised by the assembler with the DTRs located in the middle  
401 of the contig. In many of our own short-read-only assemblies, the przondoviruses described  
402 here were linearised in the middle of the genome, and required read mapping to identify where  
403 the DTRs may be. In T7-like phages, DNA is concatemeric and requires the assistance of  
404 terminases to cut at specific sites to package the DNA into the procapsid (9-11). Although  
405 each concatemer contains a single copy of the repeat, a second repeat is synthesised at the  
406 other end of the genome to prevent loss of genetic material (9, 12). Since the DTRs are present  
407 twice per phage genome, the number of terminal sequences is double following whole genome  
408 sequencing and are identified as a single peak of increased reads during read mapping (10-  
409 12, 55). Therefore, the DTR and by proxy, the start of the genome can be inferred from the  
410 read mapping. Moreover, due to the highly conserved nature of the genomes, all  
411 przondoviruses had almost the same starting sequence as the well-curated Enterobacteria  
412 phage K30 (accession HM480846) (67), making the beginning relatively easy to find. As a

413 result, considerable time was spent on re-orienting the short-read-only assemblies to be  
414 unidirectional and to have the same starting sequence.

415 One of the most problematic aspects using short-reads for phage assembly (both short-  
416 read-only and has part of a traditional hybrid assembly) was that the DTRs were deleted,  
417 possibly because the assemblers used deem them to be a sequencing artefact. Thus, DTRs  
418 need to be manually validated through primer walking and Sanger sequencing validation.  
419 However, this was unnecessary when using short-reads for polishing rather than for assembly.  
420 Thus, using the HYPPA workflow, the DTRs were present in the final polished assembly in the  
421 correct location at the ends and did not have to be manually added.

422 A second type of error that routinely occurred during non-HYPPA phage sequencing and  
423 assembly was the introduction of short insertions and/or deletions (indels) that were  
424 particularly noticeable in coding regions.

425 For the short-read only assemblies, many sequencing and assembly errors present in  
426 coding regions were only found upon annotation of the genomes, including frameshift errors  
427 in DNA polymerase (DNAP) and tail fibre protein genes. Often, these frameshift errors were  
428 found in homopolymer regions and were introduced during sequencing. Before using HYPPA,  
429 these frameshift errors were checked through read mapping followed by variant calling and  
430 edited accordingly. Particularly noteworthy were repeat regions of ~79 bp identified close to  
431 and sometimes within the DTR regions of seven of the ten phages (See **Development of a**  
432 **new workflow for the assembly of complete phage genomes** for description of repeats for  
433 Tokugawa), but that did not correlate with the increased reads observed in the read mapping.  
434 This suggested that these repeats were introduced in error during assembly and were  
435 confirmed to be artefacts in most phages, including Tokugawa through Sanger sequencing  
436 (see supplementary **Fig. S1**). Using HYPPA, we found that the two iterations of short-read  
437 polishing were able to correct single nucleotide polymorphisms and/or correct indels that  
438 resulted in these frameshift errors that long-read polishing was unable to resolve, particularly  
439 in homopolymer regions. POLCA was also able to correct indels that Polypolish was unable  
440 to resolve.

441 As previously described for Oda, all the przondoviruses contained adapter and barcode  
442 DNA upstream and/or downstream of the DTR regions. Initially, as we were trying to  
443 reconstruct the linear genome ends, we did not perform adapter and barcode trimming of the  
444 Nanopore reads prior to the long-read assembly. We then removed these sequences manually  
445 after assembly. To limit the amount of manual curation, Porechop can be used to trim the  
446 reads, however, when we attempted this for all the remaining przondoviruses, Porechop-  
447 mediated trimming resulted in several further errors. These included trimming bases from the  
448 beginning of the left terminal repeat and the end of the right terminal repeat, ranging from 3-  
449 18 bp in total; indels; multiple SNPs; and in some cases failure to assemble the phage genome

450 into a single contig, or at all. We would thus recommend manual removal of the  
451 adapter/barcodes rather than trimming of long-reads using Porechop, which appears to  
452 require more manual curation when compared to using raw Nanopore reads.

453 Multiple sequencing and/or assembly errors were identified in the coding regions of other  
454 phages, that again, persisted following traditional methods of phage assembly. Using trial and  
455 error, we were able to show that the HYPPA method was superior to other methods of phage  
456 assembly, whether hybrid or through using a single sequencing platform in correcting errors  
457 (see supplemental **Tables S2-S5** for all assembly details). Moreover, the HYPPA workflow  
458 required far fewer manual curation steps than traditional phage assembly methods: while long-  
459 read only assemblies were sometimes in the reverse orientation, all were linearised at the  
460 starting sequence. This is in contrast with the traditional assembly methods that required re-  
461 orienting the genomes to be unidirectional and starting at the same position, manual correction  
462 of large assembly errors such as indels, manual correction of homopolymer errors in coding  
463 regions, and in some cases, rearrangement of contigs and manual stitching the genome  
464 together, followed by primer walking and Sanger sequencing validation to determine the  
465 genome termini and DTRs.

466 Errors in homopolymer sequences and repeat regions are particularly common in long-  
467 read-only assemblies of bacterial genomes (43, 44, 49), and as we have described here, in  
468 phage genomes also. Indeed, two homopolymer errors occurred in the DNAP of Toyotomi,  
469 leading to a double frameshift error that resulted in three protein annotations. Short-read  
470 polishing can correct errors introduced during long-read-only assemblies (49), as we have  
471 demonstrated here. Similarly to using short-read data for polishing, we found that a traditional  
472 hybrid assembly using both short- and long-read data for Toyotomi also introduced large  
473 deletions in repeat regions, with assembly errors persisting, as has been described previously  
474 (44, 54). Assembly metadata showing all previous long-read-only, short-read-only, and hybrid  
475 assemblies is provided (see supplemental **Tables S2-S5**).

476 Several limitations of this study include the need for both short-read and long-read data for  
477 phage assembly, and specialised knowledge to access and install the software which is all  
478 freely available. Which polishing program used and what type of polishing (long-read versus  
479 short-read) in what order may give different results of equal validity. While we believe that the  
480 HYPPA workflow provides the most accurate phage genome possible, it still may not exactly  
481 reflect the DNA that is present within each phage capsid. Additionally, while the highly  
482 conserved nature of T7-like phages made it easier to determine the DTR starting sequence,  
483 this may not be the case for novel phages.

484  
485

486 **Phage genome characterisation and taxonomy**

487 All ten phages were dsDNA phages at 40,336-41,720 bp with a GC content of 52.40-  
488 53.06% which is slightly lower than their isolation host GC content of ~55.46-57.59% (**Table**  
489 **1, Fig. 3**). The number of predicted coding sequences within the genomes varies from 51 to  
490 58, and almost all coding sequences were found in the same orientation on the forward strand.  
491 However, five phages had one to four small hypothetical proteins found in opposite orientation.

492 We performed BLASTn on all phages to determine closest relatives in the NCBI GenBank  
493 database (as of October 2022). Based on the BLASTn results, which showed high levels of  
494 nucleotide similarity with reference phages, the phages in our collection were preliminarily  
495 assigned to the *Przondovirus* genus within the *Studievirinae* subfamily and *Autographiviridae*  
496 family, according to the currently established ICTV genus demarcation criterion of 70%  
497 nucleotide sequence similarity over the genome length to belong to the same genus (1).

498 The genomic relationships between our novel *przondoviruses* and a selection of  
499 *Autographiviridae* reference phages were explored further by conducting a nucleotide-based  
500 intergenomic similarity analysis using VIRIDIC (**Fig. 4, Table S2**). Included within the analysis  
501 were relatives within the same genus (*Przondovirus*), those within different genera but the  
502 same subfamily (*Studievirinae*), and those within different subfamilies (*Molineuxvirinae*,  
503 *Slopekvirinae*) (**Fig. 4**). These data confirmed that the *przondoviruses* from this study were  
504 within the ICTV genus demarcation criterion of 70% nucleotide sequence similarity over the  
505 genome length when compared to other *przondoviruses*. Several genera within the subfamily  
506 *Studievirinae* that were included only shared ~45-57% nucleotide sequence similarity with the  
507 *przondoviruses* in this study (**Fig. 4**).

508 Several *przondoviruses* clustered more closely together, including *Klebsiella* phages Oda,  
509 Toyotomi, Mera, Speegle, Cornelius, and Tokugawa, which were within ~98% nucleotide  
510 similarity, except Cornelius which was the most dissimilar at ~95-96% (**Fig. 4**). All  
511 aforementioned phages except Oda were isolated from the same wastewater treatment plant  
512 at different stages of the treatment process, using the same host. These phages are therefore  
513 likely to be different strains of the same new species of phage within the *Przondovirus* genus.  
514 Emom and Amrap clustered with their closest relative KP32, but also clustered together with  
515 ~92% similarity, and should be assigned to separate species (**Fig. 4**). Saitama and Whistle  
516 did not cluster closely with any other phage from our collection, possibly due to differences in  
517 their host specificity. Saitama did cluster with its closest relative *Klebsiella* phage K11, and  
518 Whistle clustered with its closest relative IME264 (**Fig. 4**). This suggests that Saitama, Emom,  
519 Amrap, and Whistle should be assigned to different species within the same genus.

520 After comparative genomic analyses, we observed that several of the closest database  
521 relatives were deposited in databases with incomplete genomes. Specifically, the incompleteness

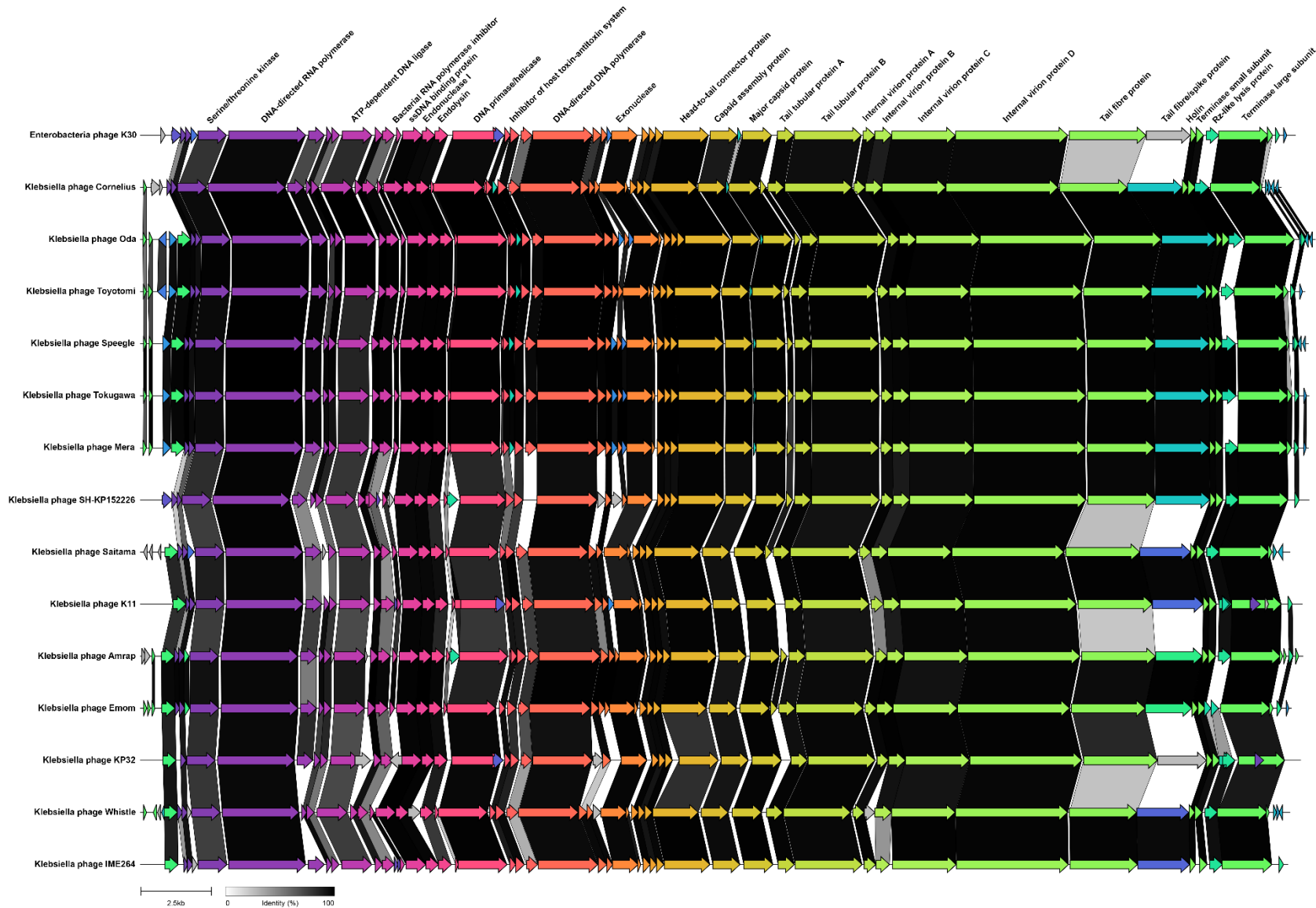


**Fig. 3. Genome map and gene clustering for przondoviruses in the collection and a selection of related phages.** Arrows represent coding sequences and pairwise comparisons of gene similarities are indicated by percentage identity given as links in greyscale, with darker shading representing areas of higher similarity. Genes without any sequence similarity are indicated without links. Some phages had a hypothetical protein following the tail fibre protein and protein BLAST revealed high homology to tail spike proteins. DTRs are present but not annotated.

484 was most often due to an absence of the DTRs, including *Klebsiella* phages KP32, KPN3, and  
485 IME264 (**Table S2**, **Fig. S2**). Incomplete genomes could lead to incorrect assignments to  
486 species in cases where the reciprocal nucleotide identities are close to the species threshold  
487 of 95% similarity across the genome length (1).

488 Additionally, potential errors were noted in phages KPN3 (accession MN101227) and KMI1  
489 (accession MN052874) (**Table S2**, **Fig. S2**). For example, KPN3 contained no annotated  
490 DNA-directed DNAP, which is conserved across all *Przondovirus* genomes analysed here.  
491 KMI1 contained a shorter DNA-directed RNAP annotation that, when included in the  
492 phylogenetic analyses, showed higher divergence, which could not be confirmed, and was  
493 therefore excluded from our phylogenetic analysis. Without raw short-read and long-read data,  
494 it is difficult to determine whether these are genuine errors or whether their differences are a  
495 true representation of the genome.

496 To further verify the taxonomic classification of the phages, phylogenetic analysis was  
497 performed using the protein sequence of the DNA-dependent RNAP, since it is the hallmark  
498 gene of the *Autographiviridae* family, using a selection of publicly available phages from the  
499 genera *Apdecimavirus*, *Berlinvirus*, *Przondovirus*, *Teetrevirus*, and *Teseptimavirus*, within the  
500 subfamily *Studiervirinae* (**Fig. 5**). As expected, the *Przondoviruses* clustered together, and there  
501 was a clear separation from other phage genera. There were some slight differences between  
502 the clustering patterns exhibited in the phylogenetic tree when compared to the VIRIDIC  
503 analysis using whole nucleotide data. *Klebsiella* phages Emom and Amrap exhibited relatively  
504 high similarity, sharing 91.5% sequence similarity across the whole nucleotide sequence, but  
505 this distinction is less obvious in the phylogenetic analysis. As observed previously (91), a  
506 single gene phylogenetic tree at the amino acid level will not provide enough resolution to  
507 accurately display within-genus relationships, leading to discrepancies between clustering of  
508 the phages Saitama, Emom, Amrap and Whistle in the VIRIDIC plot and the phylogenetic tree.

## 509 **Genome organisation and synteny**

510 We conducted comparative genomic analysis of *Przondoviruses* according to coding  
511 sequence similarity with a selection of reference phages (**Fig. 3**). We selected Enterobacteria  
512 phage K30 as the representative isolate of the *Przondovirus* genus since its genome is well-  
513 curated. *Przondoviruses* were grouped together with their closest relative according to BLASTn.  
514 As expected, all phages share a highly conserved genome organisation, which revealed a  
515 high degree of gene synteny, in concordance with the VIRIDIC data (**Fig. 4**).

516 All genomes were found to contain the early, middle, and late genes associated with viral  
517 host takeover, DNA replication, and virion assembly and lysis, respectively (**Fig. 3**). The host  
518 takeover proteins that were annotated included the S-adenosyl-L-methionine hydrolase, which  
519 is a good marker for the start of the genome; serine/threonine kinase; and DNA-directed

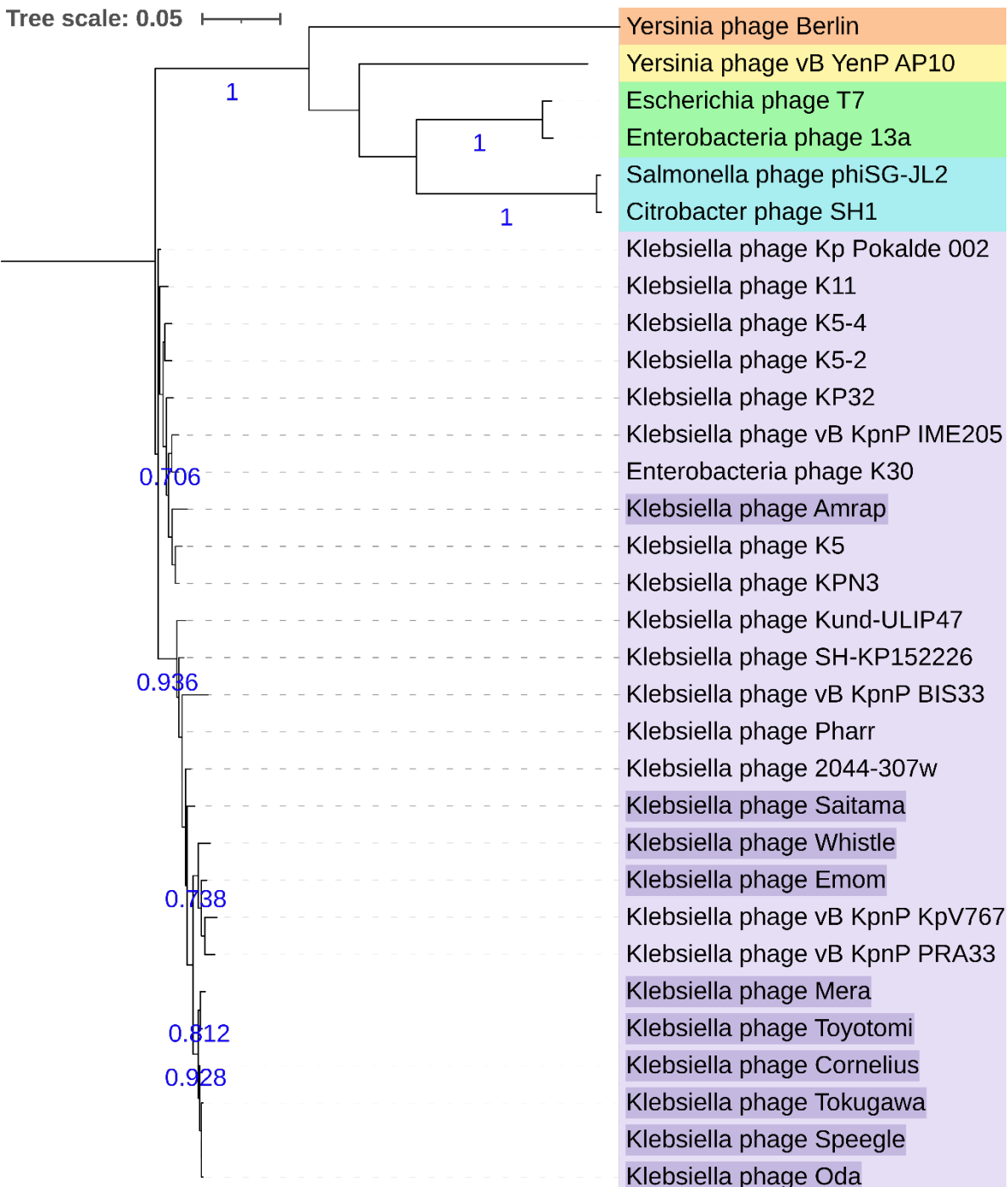


557 RNAP, with the latter being a hallmark of the *Autographiviridae* family (5, 8). The middle  
558 proteins annotated were typical for phage DNA replication. The late proteins included all the  
559 components necessary for virion assembly, such as capsid proteins and tail-associated  
560 proteins, and lysis such as holins and Rz-like lysis proteins. Of the tail-associated proteins,  
561 two tail fibre and/or spike proteins were annotated for each przondovirus.

562 Within the *Przondovirus* genus, the main differences were found in the tail proteins (**Fig.**  
563 **3**). The tail fibre and tail spike proteins are major determinants for host range, so phages that  
564 were isolated against the same *Klebsiella* host strain were expected to have higher sequence  
565 similarity across their tail fibre proteins. *Klebsiella* phages Oda, Toyotomi, Mera, Speegle,  
566 Cornelius, and Tokugawa, which were isolated against the same *K. michiganensis* strain,  
567 shared considerable sequence similarity across their entire genomes, including the tail fibre  
568 proteins. However, one difference was that Toyotomi was able to infect two hosts, whereas  
569 the remaining phages were not. This is intriguing since the high homology in the tail fibre  
570 protein would suggest similar narrow host range capabilities for this subset of przondoviruses  
571 in our collection. Emom and Amrap were both isolated against the same *K. oxytoca* strain,  
572 where they shared sequence similarity across their entire genomes, including at the tail fibre  
573 protein location. The tail fibre protein sequence similarity is complemented by the host range  
574 data for these two phages. In contrast, Cornelius and its closest relative *Klebsiella* phage SH-  
575 KP152226 still shared a high degree of sequence similarity across their entire genome,  
576 including the tail proteins, despite infecting different host species (*K. michiganensis* and *K.*  
577 *pneumoniae*, respectively). In fact, all przondoviruses in this study were found to share  
578 significant sequence similarity in their tail proteins with their closest relatives, except for  
579 Emom, and by proxy Amrap, and *Klebsiella* phage KP32. There was a lower degree of  
580 sequence similarity in the first tail fibre protein between Emom and KP32, but there was no  
581 sequence similarity in the second tail protein between Emom and that of KP32. This is possibly  
582 due to their different isolation hosts, where KP32 had been isolated against a *K. pneumoniae*  
583 strain, and Emom/Amrap were isolated against a *K. oxytoca* strain.

584 The most striking differences however, were in the tail proteins between przondoviruses in  
585 this study and reference phages that were not their closest BLASTn relatives. For example,  
586 Saitama showed sequence similarity with SH-KP152226 in only the initial part of the first tail  
587 fibre protein, with no sequence similarity exhibited elsewhere in the tail protein location. A  
588 similar pattern was observed for Emom and K11, and Whistle and KP32. This is unsurprising  
589 since the isolation host for Emom and K11 are *K. oxytoca* and *K. pneumoniae*, respectively  
590 (69, 92). Similarly, Whistle and KP32 infected two different species, *K. variicola* and *K.*  
591 *pneumoniae*, respectively. The differences in the tail fibre proteins therefore likely reflect the  
592 different isolation hosts for the przondoviruses in our collection and their database relatives.

593  
594  
595



596

597 **Fig. 5. Maximum-likelihood phylogeny of the RNAP for przondoviruses in this study and a**  
598 **selection of related Studiervirinae phages.** All phages from this study (purple highlight) clustered  
599 with related przondoviruses (purple). Outgroups, *Berlinvirus* (orange), *Apidecimavirus* (yellow),  
600 *Teseptimavirus* (green), and *Teetrevirus* (blue). Tree is midpoint rooted. Bootstrap support values at  
601  $\geq 0.7$  are given in blue (500 replicates).

602

603 Other differences between the closely related phages were found in the Rz-like lysis  
604 proteins, particularly within the przondoviruses that were within 95-98% similarity to one  
605 another. There is high sequence similarity for this protein between Cornelius and Oda, but not  
606 between Oda and Toyotomi, for example. Rz-like lysis proteins are involved in the lysis of the  
607 inner and outer membrane of Gram-negative bacteria and can be highly diverse (93-95).  
608 These proteins may be part of a single-component system, or part of a two-component system:  
609 this is where one gene may be embedded within another, overlap another, or exist as separate  
610 genes (93-95). These genes encode two different proteins that operate together to disrupt the  
611 bacterial membrane, but appear to have distinct evolutionary origins (95). The differences in  
612 membrane composition among different *Klebsiella* spp. could explain the differences in the  
613 Rz-like proteins, or may simply highlight differences between not only the proteins themselves,  
614 but the type of lysis system employed by each phage.

## 615 CONCLUSION

616 Here, we developed the HYPPA workflow for generating high quality phage genomes that  
617 require minimal manual curation, and is most representative of what is actually biologically  
618 present within the phage capsid. We tested and validated the workflow using ten  
619 przondoviruses, negating the need for laborious primer walking and Sanger sequencing  
620 validation. Accurate phage genomes provide the necessary foundation for a mechanistic  
621 understanding of infection biology, which itself is integral to the use of phages within a phage  
622 therapy setting. Moreover, accurate phage genomes provide better understanding of the  
623 nucleotide and proteomic structure and how they fit into current taxonomic classification of  
624 phages. This is particularly important when performing comparative genomic analyses. We  
625 acknowledge that the production of high-quality phage genomes using this workflow requires  
626 sequencing and bioinformatic capabilities, and may be a limiting factor for some.

## 627 FUNDING

628 CKAE is supported by the Medical Research Council (MRC) and JAFRAL as part of the  
629 Doctoral Antimicrobial Research Training (DART) MRC iCASE Programme, grant no.  
630 MR/R015937/1. TLB, AT, SKT, and EMA gratefully acknowledge funding by the Biotechnology  
631 and Biological Sciences Research Council (BBSRC); this research was funded by the BBSRC  
632 Institute Strategic Programme Gut Microbes and Health BB/R012490/1 and its constituent  
633 projects BBS/E/F/000PR10353 and BBS/E/F/000PR10356. TLV, DJB, and RE were  
634 supported by the Quadram Institute Bioscience BBSRC funded Core Capability Grant (project  
635 number BB/CCG1860/1). GT, HAK, RAK, and MAW are supported by the BBSRC Institute  
636 Strategic Programme Microbes in the Food Chain BB/R012504/1 and its constituent projects  
637 BBS/E/F/000PR10348 and BBS/E/F/000PR10349. LJH is supported by Wellcome Trust

638 Investigator Awards 100974/C/13/Z and 220876/Z/20/Z; by the BBSRC Institute Strategic  
639 Programme Gut Microbes and Health BB/R012490/1, and its constituent projects  
640 BBS/E/F/000PR10353 and BBS/E/F/000PR10356.

## 641 **AUTHOR CONTRIBUTIONS**

642 Conceptualisation: CKAE, TLB, EMA.  
643 Data curation: CKAE, TLV, RE, DJB, SKT, GT, HAK, RAK, LJH.  
644 Formal analysis: CKAE, EMA.  
645 Funding acquisition: EMA.  
646 Investigation: CKAE, TLV, GT, HAK.  
647 Methodology: CKAE, TLB, TLV, AT, EMA.  
648 Software: TLV, AT.  
649 Supervision: EMA, MAW.  
650 Validation: CKAE, TLV, EMA.  
651 Visualisation: CKAE.  
652 Writing – original draft: CKAE.  
653 Writing – review and editing: TLB, TLV, RE, DJB, AT, SKT, HAK, GT, RAK, LJH, MAW, EMA.

## 654 **ACKNOWLEDGEMENTS**

655 We would like to thank Dr Oliver Charity for assistance with comparative genomics. We  
656 gratefully acknowledge CLIMB-BIG-DATA infrastructure (MR/T030062/1) support for high-  
657 performance computing. We would like to thank Dr Kata Farkas and Prof Davey Jones at  
658 Bangor University for their assistance in procuring wastewater samples. We would like to  
659 thank Dr James Soothill at Great Ormond Street Hospital for additional clinical *Klebsiella*  
660 strains. We would like to thank all other members of the Adriaenssens Group, including Luke  
661 Acton at Quadram Institute Bioscience for their feedback and support.

## 662 **CONFLICTS OF INTEREST**

663 The authors declare that there are no conflicts of interest.

## 664 **ETHICAL STATEMENT**

665 An ethical statement for this study was not necessary since no clinical samples were  
666 processed. However, the ethical statement for the preterm infant isolates is available from the  
667 original study (25).

668

669

670 **REFERENCES**

671 1. Turner D, Kropinski AM, Adriaenssens EM. A roadmap for genome-based phage  
672 taxonomy. *Viruses*. 2021; 13(3). doi: 10.3390/v13030506.

673 2. Evseev PV, Lukianova AA, Shneider MM, Korzhenkov AA, Bugaeva EN, Kabanova  
674 AP *et al.* Origin and evolution of *Studiervirinae* bacteriophages infecting  
675 *Pectobacterium*: horizontal transfer assists adaptation to new niches. *Microorganisms*.  
676 2020; 8(11). doi: 10.3390/microorganisms8111707.

677 3. ICTV. Current ICTV Taxonomy Release. 2022. Available from:  
678 <https://ictv.global/taxonomy>. (Accessed: 04 Aug 2022).

679 4. Turner D, Shkorporov AN, Lood C, Millard AD, Dutilh BE, Alfenas-Zerbini P *et al.*  
680 Abolishment of morphology-based taxa and change to binomial species names: 2022  
681 taxonomy update of the ICTV bacterial viruses subcommittee. *Arch Virol*. 2023; 168(2):  
682 74-82. doi: 10.1007/s00705-022-05694-2.

683 5. Adriaenssens EM, Sullivan MB, Knezevic P, van Zyl LJ, Sarkar BL, Dutilh BE *et al.*  
684 Taxonomy of prokaryotic viruses: 2018-2019 update from the ICTV Bacterial and  
685 Archaeal Viruses Subcommittee. *Arch Virol*. 2020; 165(5): 1253-1260. doi:  
686 10.1007/s00705-020-04577-8.

687 6. Molineux IJ. The T7 group. In: R Calendar, ed. *The Bacteriophages*. 2nd Ed. 2006.  
688 Oxford University Press: Oxford. pp. 277-301.

689 7. Boeckman J, Korn A, Yao G, Ravindran A, Gonzalez C, Gill J. Sheep in wolves'  
690 clothing: Temperate T7-like bacteriophages and the origins of the Autographiviridae.  
691 *Virology*. 2022; 568: 86-100. doi: 10.1016/j.virol.2022.01.013.

692 8. Lavigne R, Seto D, Mahadevan P, Ackermann H-W, Kropinski AM. Unifying classical  
693 and molecular taxonomic classification: analysis of the *Podoviridae* using BLASTP-  
694 based tools. *Res Microbiol*. 2008; 159(5): 406-414. doi:  
695 <https://doi.org/10.1016/j.resmic.2008.03.005>.

696 9. Black LW. DNA packaging in dsDNA bacteriophages. *Annu Rev Microbiol*. 1989;  
697 43(1): 267-292. doi: 10.1146/annurev.mi.43.100189.001411.

698 10. Li S, Fan H, An X, Fan H, Jiang H, Chen Y *et al.* Scrutinizing virus genome termini by  
699 high-throughput sequencing. *PLoS One*. 2014; 9(1): e85806. doi:  
700 10.1371/journal.pone.0085806.

701 11. Casjens SR, Gilcrease EB. Determining DNA packaging strategy by analysis of the  
702 termini of the chromosomes in tailed-bacteriophage virions. *Methods Mol Biol*. 2009;  
703 502: 91-111. doi: 10.1007/978-1-60327-565-1\_7.

704 12. Merrill BD, Ward AT, Grose JH, Hope S. Software-based analysis of bacteriophage  
705 genomes, physical ends, and packaging strategies. *BMC Genomics*. 2016; 17(1): 679.  
706 doi: 10.1186/s12864-016-3018-2.

707 13. Guttman B, Raya R, Kutter E. Basic phage biology. In: E Kutter, A Sulakvelidze, eds.  
708 *Bacteriophages: Biology and Applications*. 2005. CRC Press: Boca Raton, Florida. pp.  
709 29-66.

710 14. Maffei E, Shaidullina A, Burkolter M, Heyer Y, Estermann F, Druelle V *et al.* Systematic  
711 exploration of *Escherichia coli* phage-host interactions with the BASEL phage  
712 collection. *PLoS Biol*. 2021; 19(11): e3001424. doi: 10.1371/journal.pbio.3001424.

713 15. Wyres KL, Lam MMC, Holt KE. Population genomics of *Klebsiella pneumoniae*. *Nat Rev Microbiol*. 2020. doi: 10.1038/s41579-019-0315-1.

715 16. Paczosa MK, Mecsas J. *Klebsiella pneumoniae*: going on the offense with a strong  
716 defense. *Microbiol Mol Biol Rev*. 2016; 80(3): 629-661. doi: 10.1128/MMBR.00078-15.

717 17. Theuretzbacher U. Global antimicrobial resistance in Gram-negative pathogens and  
718 clinical need. *Curr Opin Microbiol*. 2017; 39: 106-112. doi: 10.1016/j.mib.2017.10.028.

719 18. Theuretzbacher U, Outterson K, Engel A, Karlén A. The global preclinical antibacterial  
720 pipeline. *Nat Rev Microbiol*. 2020; 18(5): 275-285. doi: 10.1038/s41579-019-0288-0.

721 19. Kortright KE, Chan BK, Koff JL, Turner PE. Phage therapy: a renewed approach to  
722 combat antibiotic-resistant bacteria. *Cell Host Microbe*. 2019; 25(2): 219-232. doi:  
723 10.1016/j.chom.2019.01.014.

724 20. Kęsik-Szeloch A, Drulis-Kawa Z, Weber-Dąbrowska B, Kassner J, Majkowska-  
725 Skrobek G, Augustyniak D *et al.* Characterising the biology of novel lytic  
726 bacteriophages infecting multidrug resistant *Klebsiella pneumoniae*. *Virol J.* 2013; 10:  
727 100. doi: 10.1186/1743-422x-10-100.

728 21. Olsen NS, Hendriksen NB, Hansen LH, Kot W. A new high-throughput screening  
729 method for phages: enabling crude isolation and fast identification of diverse phages  
730 with therapeutic potential. *Phage.* 2020; 1(3): 137-148. doi: 10.1089/phage.2020.0016.

731 22. Carlson K. Working with bacteriophages: common techniques and methodological  
732 approaches. In: E Kutter, A Sulakvelidze, eds. *Bacteriophages: Biology and*  
733 *Applications.* 1. 2005. CRC Press: Boca Raton, Florida. pp. 437-494.

734 23. Grasis JA. Host-associated bacteriophage isolation and preparation for viral  
735 metagenomics. In: V Pantaleo, M Chiumenti, eds. *Viral Metagenomics: Methods and*  
736 *Protocols.* 2018. Springer New York: New York, New York. pp. 1-25.

737 24. Wick RR, Judd LM, Holt KE. Assembling the perfect bacterial genome using Oxford  
738 Nanopore and Illumina sequencing. *PLoS Comput Biol.* 2023; 19(3): e1010905. doi:  
739 10.1371/journal.pcbi.1010905.

740 25. Chen Y, Brook TC, Soe CZ, O'Neill I, Alcon-Giner C, Leelastwattanagul O *et al.*  
741 Preterm infants harbour diverse *Klebsiella* populations, including atypical species that  
742 encode and produce an array of antimicrobial resistance- and virulence-associated  
743 factors. *Microb Genom.* 2020. doi: 10.1099/mgen.0.000377.

744 26. Shin SH, Kim S, Kim JY, Lee S, Um Y, Oh MK *et al.* Complete genome sequence of  
745 *Enterobacter aerogenes* KCTC 2190. *J Bacteriol.* 2012; 194(9): 2373-2374. doi:  
746 10.1128/jb.00028-12.

747 27. Lee JH, Cheon IS, Shim BS, Kim DW, Kim SW, Chun J *et al.* Draft genome sequence  
748 of *Klebsiella pneumoniae* subsp. *pneumoniae* DSM 30104T. *J Bacteriol.* 2012;  
749 194(20): 5722-5723. doi: 10.1128/jb.01388-12.

750 28. Woodford N, Zhang J, Warner M, Kaufmann ME, Matos J, Macdonald A *et al.* Arrival  
751 of *Klebsiella pneumoniae* producing KPC carbapenemase in the United Kingdom. *J*  
752 *Antimicrob Chemother.* 2008; 62(6): 1261-1264. doi: 10.1093/jac/dkn396.

753 29. Chen M, Li Y, Li S, Tang L, Zheng J, An Q. Genomic identification of nitrogen-fixing  
754 *Klebsiella variicola*, *K. pneumoniae* and *K. quasipneumoniae*. *J Basic Microbiol.* 2016;  
755 56(1): 78-84. doi: 10.1002/jobm.201500415.

756 30. Schwengers O, Hoek A, Fritzenwanker M, Falgenhauer L, Hain T, Chakraborty T *et al.*  
757 ASA<sup>3</sup>P: An automatic and scalable pipeline for the assembly, annotation and higher-  
758 level analysis of closely related bacterial isolates. *PLoS Comput Biol.* 2020; 16(3):  
759 e1007134. doi: 10.1371/journal.pcbi.1007134.

760 31. Petit RA, 3rd, Read TD. Bactopia: a flexible pipeline for complete analysis of bacterial  
761 genomes. *mSystems.* 2020; 5(4). doi: 10.1128/mSystems.00190-20.

762 32. Jolley KA, Bliss CM, Bennett JS, Bratcher HB, Brehony C, Colles FM *et al.* Ribosomal  
763 multilocus sequence typing: universal characterization of bacteria from domain to  
764 strain. *Microbiology.* 2012; 158(4): 1005-1015. doi: 10.1099/mic.0.055459-0.

765 33. Jolley KA, Bray JE, Maiden MCJ. Open-access bacterial population genomics: BIGSdb  
766 software, the PubMLST.org website and their applications. *Wellcome Open Res.* 2018;  
767 3: 124. doi: 10.12688/wellcomeopenres.14826.1.

768 34. Lam MMC, Wick RR, Watts SC, Cerdeira LT, Wyres KL, Holt KE. Genomic surveillance  
769 framework and global population structure for *Klebsiella pneumoniae*. [Pre-print].  
770 2021. Doi: 10.1101/2020.12.14.422303.

771 35. Wick RR, Heinz E, Holt KE, Wyres KL. Kaptive Web: user-friendly capsule and  
772 lipopolysaccharide serotype prediction for *Klebsiella* genomes. *J Clin Microbiol.* 2018;  
773 56(6). doi: 10.1128/JCM.00197-18.

774 36. Van Twent R, Kropinski AM. Bacteriophage enrichment from water and soil. *Methods*  
775 *Mol Biol.* 2009; 501: 15-21. doi: 10.1007/978-1-60327-164-6\_2.

776 37. Kropinski AM, Mazzocco A, Waddell TE, Lingohr E, Johnson RP. Enumeration of  
777 bacteriophages by double agar overlay plaque assay. *Methods Mol Biol.* 2009; 501:  
778 69-76. doi: 10.1007/978-1-60327-164-6\_7.

779 38. Kutter E. Phage host range and efficiency of plating. In: E Kutter, A Sulakvelidze, eds. 780 *Bacteriophages: Biology and Applications*. 2005. CRC Press: Boca Raton, Florida. pp. 781 141-149.

782 39. Andrews S. FastQC: a quality control tool for high throughput sequence data. 2010. 783 Available from: <http://www.bioinformatics.babraham.ac.uk/projects/fastqc/>. (Accessed: 784 08 Jan 2021).

785 40. Chen S, Zhou Y, Chen Y, Gu J. fastp: an ultra-fast all-in-one FASTQ preprocessor. 786 *Bioinformatics*. 2018; 34(17): i884-i890. doi: 10.1093/bioinformatics/bty560.

787 41. De Coster W, D'Hert S, Schultz DT, Cruts M, Van Broeckhoven C. NanoPack: 788 visualizing and processing long-read sequencing data. *Bioinformatics*. 2018; 34(15): 789 2666-2669. doi: 10.1093/bioinformatics/bty149.

790 42. Lin Y, Yuan J, Kolmogorov M, Shen MW, Chaisson M, Pevzner PA. Assembly of long 791 error-prone reads using de Bruijn graphs. *Proc Natl Acad Sci USA*. 2016; 113(52): 792 E8396-E8405. doi: 10.1073/pnas.1604560113.

793 43. Wick R, Holt K. Benchmarking of long-read assemblers for prokaryote whole genome 794 sequencing. *F1000Research*. 2021; 8(2138). doi: 10.12688/f1000research.21782.4.

795 44. Wick RR, Judd LM, Cerdeira LT, Hawkey J, Méric G, Vezina B et al. Trycycler: 796 consensus long-read assemblies for bacterial genomes. *Genome Biol.* 2021; 22(1): 797 266. doi: 10.1186/s13059-021-02483-z.

798 45. Chen Y, Zhang Y, Wang AY, Gao M, Chong Z. Accurate long-read *de novo* assembly 799 evaluation with Inspector. *Genome Biology*. 2021; 22(1): 312. doi: 10.1186/s13059- 800 021-02527-4.

801 46. Koren S, Walenz BP, Berlin K, Miller JR, Bergman NH, Phillippy AM. Canu: scalable 802 and accurate long-read assembly via adaptive k-mer weighting and repeat separation. 803 *Genome Res.* 2017; 27(5): 722-736. doi: 10.1101/gr.215087.116.

804 47. Wick RR. Porechop. 2018. Available from: <https://github.com/rrwick/Porechop>. 805 (Accessed: 28 Oct 2022).

806 48. Wright C, Wykes M. Medaka. 2020. Available from: 807 <https://github.com/nanoporetech/medaka>. (Accessed: 22 Sep 2022).

808 49. Wick RR, Holt KE. Polypolish: short-read polishing of long-read bacterial genome 809 assemblies. *PLoS Comput Biol.* 2022; 18(1): e1009802. doi: 10.1371/journal.pcbi.1009802.

810 50. Zimin AV, Salzberg SL. The genome polishing tool POLCA makes fast and accurate 811 corrections in genome assemblies. *PLoS Comput Biol.* 2020; 16(6): e1007981. doi: 812 10.1371/journal.pcbi.1007981.

813 51. Seemann T. Shovill. 2018. Available from: <https://github.com/tseemann/shovill>. 814 (Accessed: 12 Jan 2021).

815 52. Bankevich A, Nurk S, Antipov D, Gurevich AA, Dvorkin M, Kulikov AS et al. SPAdes: 816 a new genome assembly algorithm and its applications to single-cell sequencing. *J 817 Comput Biol.* 2012; 19(5): 455-477. doi: 10.1089/cmb.2012.0021.

818 53. Walker BJ, Abeel T, Shea T, Priest M, Abouelhail A, Sakthikumar S et al. Pilon: an 819 integrated tool for comprehensive microbial variant detection and genome assembly 820 improvement. *PLoS One*. 2014; 9(11): e112963. doi: 10.1371/journal.pone.0112963.

821 54. Wick RR, Judd LM, Gorrie CL, Holt KE. Unicycler: resolving bacterial genome 822 assemblies from short and long sequencing reads. *PLoS Comput Biol.* 2017; 13(6): 823 e1005595. doi: 10.1371/journal.pcbi.1005595.

824 55. Garneau JR, Depardieu F, Fortier LC, Bikard D, Monot M. PhageTerm: a tool for fast 825 and accurate determination of phage termini and packaging mechanism using next- 826 generation sequencing data. *Sci Rep.* 2017; 7(1): 8292. doi: 10.1038/s41598-017- 827 07910-5.

828 56. Benes V, Kilger C, Voss H, Pääbo S, Ansorge W. Direct primer walking on P1 plasmid 829 DNA. *BioTechniques*. 1997; 23(1): 98-100.

830 57. Wood DE, Lu J, Langmead B. Improved metagenomic analysis with Kraken 2. *Genome 831 Biol.* 2019; 20(1): 257-269. doi: 10.1186/s13059-019-1891-0.

832

833 58. Langmead B, Salzberg SL. Fast gapped-read alignment with Bowtie 2. *Nat Methods*.  
834 2012; 9(4): 357-359. doi: 10.1038/nmeth.1923.

835 59. Thorvaldsdottir H, Robinson JT, Mesirov JP. Integrative Genomics Viewer (IGV): high-  
836 performance genomics data visualization and exploration. *Brief Bioinform*. 2013; 14(2):  
837 178-192. doi: 10.1093/bib/bbs017.

838 60. Grubaugh ND, Gangavarapu K, Quick J, Matteson NL, De Jesus JG, Main BJ *et al*. An  
839 amplicon-based sequencing framework for accurately measuring intrahost virus  
840 diversity using PrimalSeq and iVar. *Genome Biol*. 2019; 20(1): 8. doi: 10.1186/s13059-  
841 018-1618-7.

842 61. Li H, Durbin R. Fast and accurate short read alignment with Burrows-Wheeler  
843 transform. *Bioinformatics*. 2009; 25(14): 1754-1760. doi:  
844 10.1093/bioinformatics/btp324.

845 62. Li H. Aligning sequence reads, clone sequences and assembly contigs with BWA-  
846 MEM. [Pre-print]. 2013. Doi: 10.48550/ARXIV.1303.3997.

847 63. Okonechnikov K, Golosova O, Fursov M, team tU. Unipro UGENE: a unified  
848 bioinformatics toolkit. *Bioinformatics*. 2012; 28(8): 1166-1167.

849 64. Bouras G, Nepal R, Houtak G, Psaltis AJ, Wormald P-J, Vreugde S. Pharokka: a fast  
850 scalable bacteriophage annotation tool. *Bioinformatics*. 2022; 39(1). doi:  
851 10.1093/bioinformatics/btac776.

852 65. McNair K, Zhou C, Dinsdale EA, Souza B, Edwards RA. PHANOTATE: a novel  
853 approach to gene identification in phage genomes. *Bioinformatics*. 2019; 35(22): 4537-  
854 4542. doi: 10.1093/bioinformatics/btz265.

855 66. Hsieh PF, Lin HH, Lin TL, Chen YY, Wang JT. Two T7-like bacteriophages, K5-2 and  
856 K5-4, each encodes two capsule depolymerases: isolation and functional  
857 characterization. *Sci Rep*. 2017; 7(1): 4624. doi: 10.1038/s41598-017-04644-2.

858 67. Whitfield C, Lam M. Characterisation of coliphage K30, a bacteriophage specific for  
859 *Escherichia coli* capsular serotype K30. *FEMS Microbiol Lett*. 1986; 37(3): 351-355.  
860 doi: 10.1111/j.1574-6968.1986.tb01823.x.

861 68. Teng T, Li Q, Liu Z, Li X, Liu Z, Liu H *et al*. Characterization and genome analysis of  
862 novel *Klebsiella* phage Henu1 with lytic activity against clinical strains of *Klebsiella*  
863 *pneumoniae*. *Arch Virol*. 2019; 164(9): 2389-2393. doi: 10.1007/s00705-019-04321-x.

864 69. Rudolph C, Freund-Mölbert E, Stirm S. Fragments of *Klebsiella* bacteriophage no. 11.  
865 *Virology*. 1975; 64(1): 236-246. doi: 10.1016/0042-6822(75)90095-1.

866 70. Thiry D, Passet V, Danis-Włodarczyk K, Lood C, Wagemans J, De Sordi L *et al*. New  
867 bacteriophages against emerging lineages ST23 and ST258 of *Klebsiella pneumoniae*  
868 and efficacy assessment in *Galleria mellonella* larvae. *Viruses*. 2019; 11(5): E411. doi:  
869 10.3390/v11050411.

870 71. Wu Y, Wang R, Xu M, Liu Y, Zhu X, Qiu J *et al*. A novel polysaccharide depolymerase  
871 encoded by the phage SH-KP152226 confers specific activity against multidrug-  
872 resistant *Klebsiella pneumoniae* via biofilm degradation. *Front Microbiol*. 2019; 10:  
873 2768. doi: 10.3389/fmicb.2019.02768.

874 72. Labudda Ł, Strapagiel D, Karczewska-Golec J, Golec P. Complete annotated genome  
875 sequences of four *Klebsiella pneumoniae* phages isolated from sewage in Poland.  
876 *Genome Announc*. 2017; 5(45). doi: 10.1128/genomeA.00919-17.

877 73. Liu Y, Leung SSY, Huang Y, Guo Y, Jiang N, Li P *et al*. Identification of two  
878 depolymerases from phage IME205 and their antivirulent functions on K47 capsule of  
879 *Klebsiella pneumoniae*. *Front Microbiol*. 2020; 11: 218. doi:  
880 10.3389/fmicb.2020.00218.

881 74. Kwon HJ, Cho SH, Kim TE, Won YJ, Jeong J, Park SC *et al*. Characterization of a T7-  
882 like lytic bacteriophage (phiSG-JL2) of *Salmonella enterica* serovar Gallinarum biovar  
883 Gallinarum. *Appl Environ Microbiol*. 2008; 74(22): 6970-6979. doi:  
884 10.1128/aem.01088-08.

885 75. Hamdi S, Rousseau GM, Labrie SJ, Kourda RS, Tremblay DM, Moineau S *et al*.  
886 Characterization of five *Podoviridae* phages infecting *Citrobacter freundii*. *Front  
887 Microbiol*. 2016; 7: 1023. doi: 10.3389/fmicb.2016.01023.

888 76. Blierot I, Blasco L, Pacios O, Fernández-García L, Ambroa A, López M *et al.* The role  
889 of PemIK (PemK/PemI) type II TA system from *Klebsiella pneumoniae* clinical strains  
890 in lytic phage infection. *Sci Rep.* 2022; 12(1): 4488. doi: 10.1038/s41598-022-08111-  
891 5.

892 77. Dunn JJ, Studier FW. Complete nucleotide sequence of bacteriophage T7 DNA and  
893 the locations of T7 genetic elements. *J Mol Biol.* 1983; 166(4): 477-535. doi:  
894 10.1016/s0022-2836(83)80282-4.

895 78. Dobbins AT, George M, Jr., Basham DA, Ford ME, Houtz JM, Pedulla ML *et al.*  
896 Complete genomic sequence of the virulent *Salmonella* bacteriophage SP6. *J  
897 Bacteriol.* 2004; 186(7): 1933-1944. doi: 10.1128/jb.186.7.1933-1944.2004.

898 79. McGinnis S, Madden TL. BLAST: at the core of a powerful and diverse set of sequence  
899 analysis tools. *Nucleic Acids Res.* 2004; 32(Web server issue): W20-W25. doi:  
900 10.1093/nar/gkh435.

901 80. Darling AE, Mau B, Perna NT. progressiveMauve: multiple genome alignment with  
902 gene gain, loss and rearrangement. *PLoS One.* 2010; 5(6): e11147. doi:  
903 10.1371/journal.pone.0011147.

904 81. Moraru C, Varsani A, Kropinski AM. VIRIDIC - a novel tool to calculate the  
905 intergenomic similarities of prokaryote-infecting viruses. *Viruses.* 2020; 12(11): 1268.  
906 doi: 10.3390/v12111268.

907 82. Kumar S, Stecher G, Li M, Knyaz C, Tamura K. MEGA X: Molecular evolutionary  
908 genetics analysis across computing platforms. *Mol Biol Evol.* 2018; 35(6): 1547-1549.  
909 doi: 10.1093/molbev/msy096.

910 83. Letunic I, Bork P. Interactive tree of life (iTOL) v5: an online tool for phylogenetic tree  
911 display and annotation. *Nucleic Acids Res.* 2021. doi: 10.1093/nar/gkab301.

912 84. Gilchrist CLM, Chooi Y-H. Clinker & clustermap.js: automatic generation of gene  
913 cluster comparison figures. *Bioinformatics.* 2021; 37(16): 2473-2475. doi:  
914 10.1093/bioinformatics/btab007.

915 85. Nobrega FL, Vlot M, de Jonge PA, Dreesens LL, Beaumont HJE, Lavigne R *et al.*  
916 Targeting mechanisms of tailed bacteriophages. *Nat Rev Microbiol.* 2018; 16(12): 760-  
917 773. doi: 10.1038/s41579-018-0070-8.

918 86. González-García VA, Pulido-Cid M, Garcia-Doval C, Bocanegra R, van Raaij MJ,  
919 Martín-Benito J *et al.* Conformational changes leading to T7 DNA delivery upon  
920 interaction with the bacterial receptor. *J Biol Chem.* 2015; 290(16): 10038-10044. doi:  
921 10.1074/jbc.M114.614222.

922 87. Latka A, Maciejewska B, Majkowska-Skrobek G, Briers Y, Drulis-Kawa Z.  
923 Bacteriophage-encoded virion-associated enzymes to overcome the carbohydrate  
924 barriers during the infection process. *Appl Microbiol Biotechnol.* 2017; 101(8): 3103-  
925 3119. doi: 10.1007/s00253-017-8224-6.

926 88. Eskenazi A, Lood C, Wubbolts J, Hites M, Balarjishvili N, Leshkasheli L *et al.*  
927 Combination of pre-adapted bacteriophage therapy and antibiotics for treatment of  
928 fracture-related infection due to pandrug-resistant *Klebsiella pneumoniae*. *Nat  
929 Commun.* 2022; 13(1): 302. doi: 10.1038/s41467-021-27656-z.

930 89. Piel D, Bruto M, Labreuche Y, Blanquart F, Goudenege D, Barcia-Cruz R *et al.* Phage-  
931 host coevolution in natural populations. *Nat Microbiol.* 2022; 7(7): 1075-1086. doi:  
932 10.1038/s41564-022-01157-1.

933 90. Turner D, Adriaenssens EM, Tolstoy I, Kropinski AM. Phage annotation guide:  
934 guidelines for assembly and high-quality annotation. *Phage (New Rochelle).* 2021;  
935 2(4): 170-182. doi: 10.1089/phage.2021.0013.

936 91. Barylski J, Enault F, Dutilh BE, Schuller MB, Edwards RA, Gillis A *et al.* Analysis of  
937 Spounaviruses as a case study for the overdue reclassification of tailed phages. *Syst  
938 Biol.* 2020; 69(1): 110-123. doi: 10.1093/sysbio/syz036.

939 92. Pan YJ, Lin TL, Chen CT, Chen YY, Hsieh PF, Hsu CR *et al.* Genetic analysis of  
940 capsular polysaccharide synthesis gene clusters in 79 capsular types of *Klebsiella* spp.  
941 *Sci Rep.* 2015; 5: 15573. doi: 10.1038/srep15573.

942 93. Summer EJ, Berry J, Tran TAT, Niu L, Struck DK, Young R. Rz/Rz1 lysis gene  
943 equivalents in phages of Gram-negative hosts. *J Mol Biol.* 2007; 373(5): 1098-1112.  
944 doi: 10.1016/j.jmb.2007.08.045.

945 94. Berry J, Summer EJ, Struck DK, Young R. The final step in the phage infection cycle:  
946 the Rz and Rz1 lysis proteins link the inner and outer membranes. *Mol Microbiol.* 2008;  
947 70(2): 341-351. doi: 10.1111/j.1365-2958.2008.06408.x.

948 95. Kongari R, Rajaure M, Cahill J, Rasche E, Mijalis E, Berry J *et al.* Phage spanins:  
949 diversity, topological dynamics and gene convergence. *BMC Bioinformatics.* 2018;  
950 19(1): 326. doi: 10.1186/s12859-018-2342-8.

951